Geophysical Journal International

Geophys. J. Int. (2015) **202,** 1453–1462 doi: 10.1093/gji/ggv211
GJI Seismology

Influence of the continental margin on the stress field and seismicity in the intraplate Acaraú Seismic Zone, NE Brazil

Paulo H.S. Oliveira,[1] Joaquim M. Ferreira,[2,3] Francisco H.R. Bezerra,[2,4] Marcelo Assumpção,[5] Aderson F. do Nascimento,[2,3] Maria O.L. Sousa[4] and Eduardo A.S. Menezes[3]

[1] *Escola de Ciências e Tecnologia, Universidade Federal do Rio Grande do Norte, Brazil*
[2] *Programa de Pós – Graduação em Geodinâmica e Geofísica, Universidade Federal do Rio Grande do Norte, Brazil. E-mail: joaquim@geofisica.ufrn.br*
[3] *Departamento de Geofísica, Universidade Federal do Rio Grande do Norte, Brazil*
[4] *Departamento de Geologia, Universidade Federal do Rio Grande do Norte, Brazil*
[5] *Departamento de Geofísica, Instituto de Astronomia, Geofísica e Ciências Atmosféricas, Universidade de São Paulo, Brazil*

Accepted 2015 May 19. Received 2015 May 18; in original form 2015 January 12

SUMMARY

The Borborema province in NE Brazil is characterized by seismic sequences with small earthquakes that can last 10 yr or more. The seismicity in this region is concentrated in three main seismic zones. In this work, we investigate the stress field in one of these zones, the Acaraú Seismic Zone, which is located in the NW part of the Borborema province. This seismic zone exhibits earthquake sequences that contain repeated earthquakes with similar waveforms and a shallow depth. Using a local network, we investigated a seismic sequence close to the town of Santana do Acaraú from December 2009 to December 2010, and we present detailed results (velocity model, hypocentres and focal mechanism) from this network. In addition, we inverted seven focal mechanisms, including six that were used in previous studies, and determined the directions of the three main axes of the regional stress field. Selecting a very precise set of 12 earthquakes, we found an active seismic zone with a depth between 3.5 and 4.8 km and with a horizontal dimension of approximately 2.5 km in the NW–SE direction (azimuth of 118°) and a strike-slip focal mechanism. The new seismic fault and some of the previous seismic faults determined in previous studies occur near the continental-scale Transbrasiliano lineament, but they exhibit no direct relationship with that ancient structure. The stress field is characterized by NW–SE trending compression and NE–SW trending extension. This result suggests that the rheological contrast between the continental–oceanic crusts created flexural stresses with maximum horizontal compression parallel to the continental margin. This stress pattern occurs along the Potiguar basin and continues west as far as the Amazon fan along the Equatorial margin of Brazil. This stress field and related seismicity may be a characteristic of this type of passive margin that is generated during the transform shearing between the South America and Africa plates and that exhibits an abrupt oceanic–continent transition, steep continental slopes and high bathymetric gradients.

Key words: Earthquake source observations; Seismicity and tectonics; Continental neotectonics.

1 INTRODUCTION

Two major issues have been emphasized in the debate of the seismicity in intraplate areas. The first issue is the stress field, which is characterized by compressive stress regimes with maximum compression dominantly oriented parallel to absolute plate motions in intraplate regions, including important variations across large areas (Zoback 1992). In the intraplate South America, the maximum horizontal stress (SHmax) is uniformly oriented E–W. However, there are some local deviations from the regional pattern. For example, the direction of the compressional stresses appears to rotate from E–W in Eastern Brazil and northern Argentina to approximately NW–SE in the Amazon region, which can be explained by numerical models of continental-scale plate-boundary forces (Assumpção 1992). Along the Equatorial margin of NE Brazil (Fig. 1), the maximum horizontal compression is roughly parallel to the coast, which

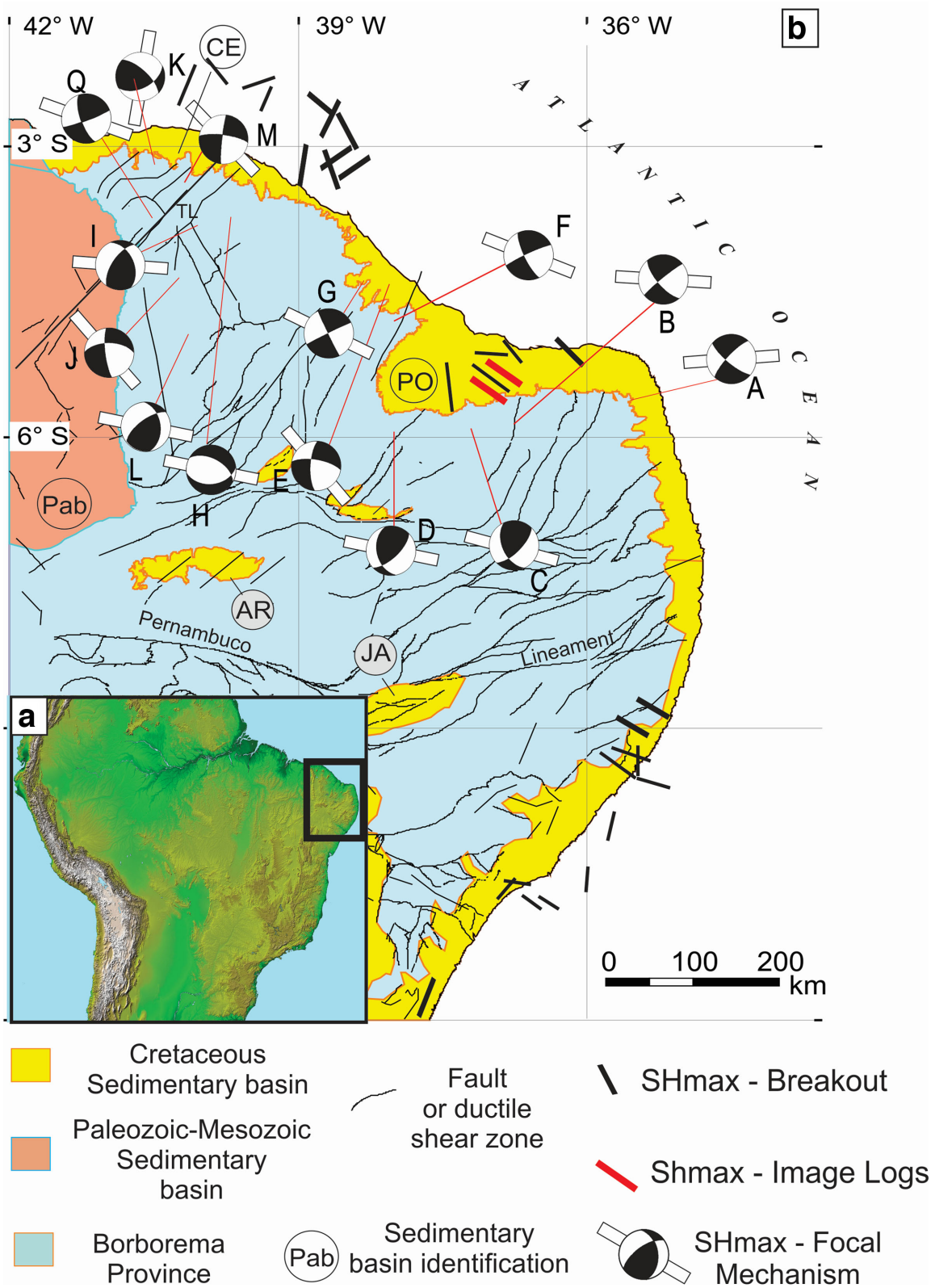

Figure 1. (a) Inset: the South American continent; (b) simplified seismo-tectonic map of the Borborema Province with emphasis on the stress field along the equatorial (northern) margin of Brazil. Sedimentary basins: AR, Araripe; PO, Potiguar; Pab, Parnaíba; JA, Jatobá; CE, Ceará. Location and year of the focal mechanisms: A, João Câmara (Ferreira *et al.* 1998); B, Açu (Ferreira *et al.* 1998); C, Augusto Severo (Ferreira *et al.* 1998); D, Tabuleiro Grande (Ferreira *et al.* 1998); E, Palhano (Ferreira *et al.* 1998); F, Pacajus (Ferreira *et al.* 1998); G, Cascavel (Ferreira *et al.* 1998); H, I, Irauçuba (Ferreira *et al.* 1998); J, Groaíras (Ferreira *et al.* 1998); K, Senador Sá (França *et al.* 2004); L, Hidrolândia (Ferreira *et al.* 1998); M, Santana do Acaraú (this paper), Q, Serra da Meruoca (Oliveira *et al.* 2010).

indicates a combination of regional stress sources (asthenospheric drag and ridge push) with local sources (Assumpção 1992; Ferreira *et al.* 1998).

The second issue is the location of the source of intraplate seismicity. Intraplate seismicity has been explained in terms of stress concentration, reactivation of pre-existing zones of weakness, or both (Sykes 1978; Johnston 1989; Talwani 2014). In intraplate South America, the continental margin is more seismically active than the average intraplate region (Assumpção *et al.* 2014), which may indicate that the continental margin has some control over the occurrence of intraplate events. Along this margin, the Borborema province (Bp) in northeastern Brazil is the most seismically active area (Fig. 1; Assumpção *et al.* 2014); three main seismic zones have been identified: (1) along the eastern part of the Pernambuco lineament (Ferreira *et al.* 2008; Lopes *et al.* 2010; Lima Neto *et al.* 2014), (2) in the crystalline basement around the Bp (Ferreira *et al.* 1998; Bezerra *et al.* 2011; Reis *et al.* 2013) and (3) in the Acaraú Seismic Zone (ASZ) in the northwestern part of the Borborema province, close to the Parnaíba Basin (Ferreira *et al.* 1998; França *et al.* 2004; Moura *et al.* 2014). The maximum magnitude event in the region was the 1980, 5.2 m_b Pacajus earthquake with MM intensity VII, which was located in the western part of the Potiguar basin (seismic zone 2, Ferreira *et al.* 1998). However, the seismic sequences could last a decade or more, and the events are confined to the upper brittle crust with a depth ranging from 1 to 12 km.

Knowledge of the stress field and seismicity in intraplate South America is important for understanding the mechanisms of the intraplate seismicity and regional neotectonic deformation. Despite being geographically situated in the stable continental region of the South American Plate, Brazil has areas with important sources of intraplate earthquakes, such as northeastern and southeastern regions.

The models of intraplate stress in South America still require complementary data. For example, the maximum horizontal stress roughly follows the shoreline geometry in the Equatorial margin of the Borborema Province (Fig. 1), indicating that local features, such as the flexural stresses, influence the local (scale $<$100 km) stress pattern (Assumpção 1992; Ferreira *et al.* 1998; Reis *et al.* 2013). However, additional studies are needed to validate or rule out these existing models.

The intraplate South America has a short historical record and sparse palaeoseismic studies, which is similar to intraplate Australia (Sandiford & Egholm 2008). These studies could be used to address these problems. However, new and better seismic data have accumulated over the past decades, and new questions about the origin and characteristics of intraplate earthquakes and stress field have emerged. For example, the association of intraplate events with rift structures has been described, such as in the New Madrid Seismic Zone (Van Arsdale 2014). Nevertheless, the identification of causal seismogenic structures within rifts has been elusive (Talwani 2014). Therefore, there are significant uncertainties regarding the long-term patterns of seismicity, sources of stress and intraplate events.

This paper describes the results of hypocenters and focal mechanism in the ASZ, close to the Equatorial margin (Fig. 1), where an earthquake sequence was recorded with six digital stations that operated from December 2009 to December 2010. This margin is characterized by events up to 5.2 m_b, with MM intensity VII and earthquake sequences with small events that can last 10 yr or more. Earthquakes are confined at the upper crust with a depth ranging from 1 to 12 km (Ferreira *et al.* 1998). We determined the main characteristics of the seismogenic faults, and we used data from six other focal mechanisms in previous studies to determine the regional stress field. The main problems we address in ASZ are as follows: (1) the relationship between the regional stress field and the Equatorial margin and (2) the relationship (or lack thereof) between the seismogenic fault and pre-existing Precambrian fabric and rift faults. Our study may have implications for understanding the influence of continental margins on both the stress field and seismicity.

2 GEOLOGIC AND TECTONIC FRAMEWORK OF THE NORTHERN PART OF THE BORBOREMA PROVINCE

2.1 Geology of the northern part of the Borborema province

The Equatorial margin of Brazil was formed in the Mesozoic during the breakup between Africa and South America. This breakup occurred along a right-lateral major zone at ∼140 Ma, when several grabens were formed (Matos 1992, 2000). Three major basins formed in the eastern part of the Equatorial margin in Brazil: the Potiguar, Ceará, and Barreirinhas (Fig. 1). The Potiguar basin is the most well-known of these basins, and it had two rift phases. The first was in the early Cretaceous age, which formed a normal fault system oriented NE–SW and is related to extensional tectonic stresses. The second was in the medium Cretaceous, which is related to the onset of the continental drift (Matos 1992). The Potiguar Basin consists of a continental rift unit deposited in the Neocomian, a post-rift transitional unit deposited in the Aptian, and a drift unit deposited from the Albian.

The ASZ mainly consists of a Precambrian crystalline basement and Palaeozoic sedimentary basins. The crystalline basement primarily consists of Archean and Proterozoic units deformed during the Brasiliano-Pan African orogeny (740–560 Ma, Fetter *et al.* 1997; Brito Neves *et al.* 2014). These terrains are deformed by E–W- to NE–SW-striking, large-scale, strike-slip and thrust shear zones of late Neoproterozoic age (Santos *et al.* 2008; Fig. 2). The Jaibaras basin is an elongated NE–SW-trending structure extending to the southwest beneath the sedimentary rocks of the Parnaíba basin, and it was formed in the Eopalaeozoic during the Palaeozoic and Mesozoic (Oliveira & Mohriak 2003, Fig. 2). This basin represents the brittle reactivation of the Transbrasiliano lineament, a major strike-slip Precambrian shear zone that cut across South America and continues into Africa (De Castro *et al.* 2014).

2.2 Seismicity and stress field in the northern part of the Borborema province

The earthquake sequence studied in this paper is concentrated on the NW border of the Borborema province (Fig. 1). The Borborema province is one of the most seismically active regions of intraplate South America (Assumpção *et al.* 2014). Seismic activity in this region is concentrated in the following three areas: (1) near the Pernambuco lineament (Ferreira *et al.* 2008; Lopes *et al.* 2010; Lima Neto *et al.* 2014), (2) in the crystalline basement around the Potiguar basin (Ferreira *et al.* 1998; Bezerra *et al.* 2007), and (3) in the Acaraú Seismic Zone in the northwestern border of the province (Ferreira *et al.* 1998; França *et al.* 2004; Oliveira *et al.* 2010).

The ASZ has a 200-yr record of historical and instrumental seismicity. The first event felt in this seismic zone was the Granja in the 1810 earthquake (Ferreira & Assumpção 1983). More recently,

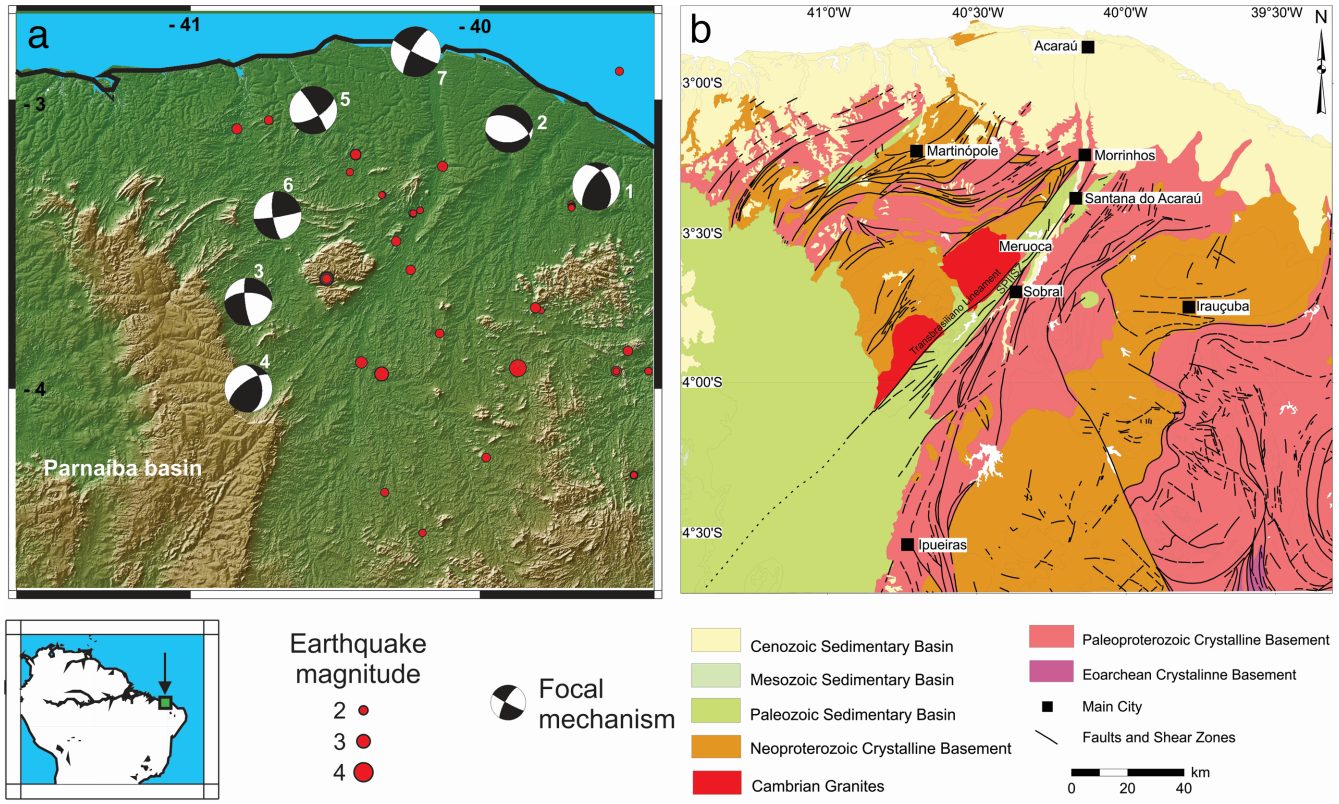

Figure 2. (a) Focal mechanisms of the Acaraú seismic zone in the northwestern part of the Borborema Province. The red circle indicates epicentral location of the earthquakes. Inset: the South American continent. Focal mechanisms: 1 and 2 – Irauçuba (1991); 3 – Groaíras (1988); 4 – Hidrolândia (1991) (Ferreira *et al.* 1998); 5 – Senador Sá (1998) (França *et al.* 2004); 6 – Serra da Meruoca (2008) (Oliveira *et al.* 2010) and 7 – Santana do Acaraú (2010) (this study). (b) Geological map of study area (simplified from Santos *et al.* 2008).

several seismic sequences were monitored with local seismic stations, generally after moderate events. The following focal mechanisms represent these seismic sequences, which occurred in different years and locations (Fig. 2): 1 and 2 – Irauçuba (1991), 3 – Groaíras (1988), 4 – Hidrolândia (1991; Ferreira *et al.* 1998), 5 – Senador Sá (1998; França *et al.* 2004), 6 – Serra da Meruoca (2008; Oliveira *et al.* 2010) and 7 – Santana do Acaraú (this study).

The present-day stress regime along the northern part of the Borborema province, which corresponds to the Equatorial margin, was derived from focal mechanisms (Ferreira *et al.* 1998), borehole breakout (Lima *et al.* 1997), and image logs (Reis *et al.* 2013). These data indicate that the maximum horizontal compression trends E–W in the eastern part of the Potiguar basin, and it shifts to NW–SE in the central and western part of the basin, roughly parallel to the coastline. Image logs also indicate that the stress field changes from a normal stress regime from 0 to 2.5 km to a strike-slip/normal regime below 2.5 km. The stress axis $\sigma 1$ rotates from vertical to a subhorizontal position parallel to the shoreline (Reis *et al.* 2013). This is consistent with the focal mechanisms of the basement from a depth of 1 to 9 km, indicating mainly strike-slip faulting at considerable depths (Ferreira *et al.* 1998; Bezerra *et al.* 2007).

3 DATA AND PROCESSING

The network deployed in the study area (SA network) operated with six stations for two periods: 2009 December 19 to 2010 March 07 (Network 1) and 2010 October 8 to December 28 (Network 2). During this last period, the northernmost station (SAJM) was moved to the south (SAFL) to improve the epicentral determinations (Figs 6–9). Each station consisted of a triaxial short period Sercel L4C3D sensor (1 Hz) and a Reftek DAS-130 recorder with 250 Hz sampling.

A set of 450 local events was detected during the SA network operation. To verify the consistency of the readings and to determine the V_P/V_S ratio, we used a composite Wadati diagram. The Wadati diagram plots S–P versus P traveltimes. For media with a constant V_P/V_S ratio, the data should follow a straight line with a slope that is directly related to the V_P/V_S ratio of the medium. We obtained a V_P/V_S ratio of 1.701 ± 0.004. Subsequently, we searched for the best half-space *P*-wave velocity between $V_P = 5.0$ and 6.4 km s^{-1} using the HYPO71 code (Lee & Lahr 1975). The hypocentres were determined using HYPO71 with a half-space of $V_P = 6.0$ km s^{-1}.

A half-space velocity model was used because the seismographic stations were deployed over a granitic-gneissic basement (Ferreira *et al.* 1998; França *et al.* 2004; Lima Neto *et al.* 2013, 2014). This is consistent with the impulsive *P*- and *S*-wave arrivals observed in the seismograms of Fig. 3.

To improve the accuracy of the hypocentre location, we used the HYPODD code (Waldhauser & Ellsworth 2000; Waldhauser 2001) that employs the double-difference (DD algorithm). The DD technique assumes that the hypocentral distance between a pair of earthquakes is small compared to the event-station distance (Waldhauser & Ellsworth 2000).

To estimate the fault-plane orientation (azimuth and dip), we applied the least squares method to fit a single plane to more accurate

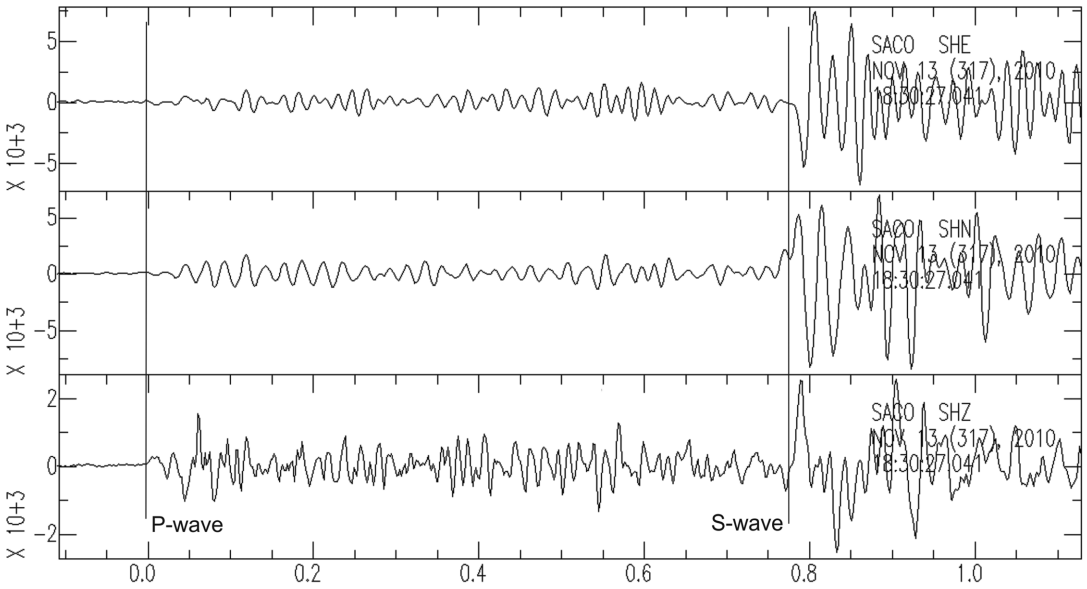

Figure 3. Seismogram of a local event recorded at five stations on 2010 November 13 showing clear *P*- and *S*-wave arrivals (vertical lines).

Table 1. Focal mechanism set used to perform the stress inversion in the Acaraú Seismic Zone, NW part of the Borborema Province.

Focal mechanism	Locality	Date	Lat (°)	Long (°)	Depth (km)	Fault plane solution			*P*-axe azimuth	Reference
						Strike (°)	Dip (°)	Rake (°)	P (°)	
1	Irauçuba (a)	1991	−3.93	−39.87	8–12	298	53	−68	265	Ferreira *et al.* (1998)
2	Irauçuba (b)	1991	–	–	–	335	45	40	278	Ferreira *et al.* (1998)
3	Groaíras	1988	−3.95	−40.34	6–11	173	78	−33	127	Ferreira *et al.* (1998)
4	Hidrolândia	1991	−4.36	−40.33	0–2	353	43	37	298	Ferreira *et al.* (1998)
5	Senador Sá	1998	−3.19	−40.43	4–5	60	65	−174	278	França *et al.* (2004)
6	Meruoca	2008	−3.62	−40.51	1–8	81	85	161	130	Oliveira *et al.* (2010)
7	Santana do Acaraú	2010	−3.38	−40.21	3–5	118	89	165	73	This paper

events. Using this fault plane, we determined the Santana do Acaraú focal mechanism with the FPFIT code (Reasenberg & Oppenheimer 1985). To ensure good results, we only used *P*-wave polarities with 100 per cent confidence and the trend of hypocentres to define the type of focal mechanism.

Considering the fault-plane solutions shown in Table 1, we used the code *gridfix* (Michael 1984, 1987) to invert seven regional focal mechanisms: six from previous studies and one from this paper. The inversion was implemented by minimizing the difference between the observed slip direction and the evaluated shear stress orientation on the fault. It is assumed that the slip direction of the earthquake rupture is given by the tectonic shear stress on the fault plane. We used a grid search with steps of 2° to determine the directions of the three main stresses (σ_1, σ_2 and σ_3).

4 RESULTS

The daily activity detected during the SA network operation (2009 December 17 to 2010 December 23) is shown in Fig. 4, and we observed some data gaps because of several technical problems. Despite these problems, we had some important observations. The Santana do Acaraú seismic activity increased and reached a peak of 45 earthquakes on 2010 March 5, and it increased again between 2010 November 10 and 25, and then decreased from 2010 December 2 to 23 (Fig. 4).

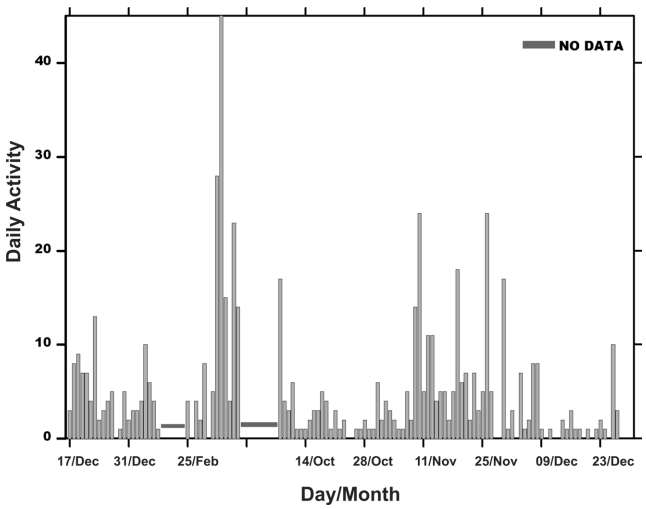

Figure 4. Temporal distribution of the Santana do Acaraú seismicity (450 events) from 2009 December 17 to 2010 December 28, as recorded by the local network. Vertical and Horizontal bars indicate the daily number of events recorded at the stations of the SA network and periods with no data, respectively.

4.1 Hypocentral determination

To ensure high-quality results, only those events with at least eight readings (4P- and 4S-readings) and with the lowest rms time residual

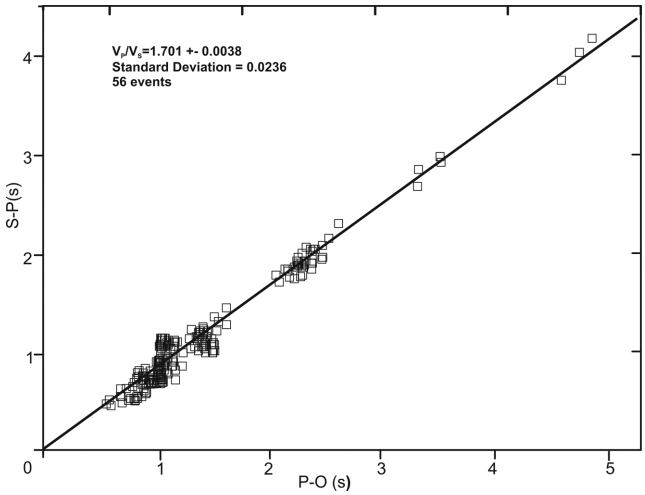

Figure 5. Composite Wadati diagram for Santana do Acaraú seismicity using 56 events (235 black squares). The best fit (solid line) indicates a ratio $V_P/V_S = 1.701$ (± 0.0038). S–P(s) are *S*-wave and *P*-wave time difference. P–O (s) is *P* wave and origin time difference.

$\leq$0.04 s were used. A Wadati diagram constructed with this readings indicates a ratio $V_P/V_S = 1.701$ (± 0.0038) for the 56 best events (Fig. 5).

Using the identified velocity model ($V_P/V_S = 1.70$ and $V_P = 6.0\,\mathrm{km\,s^{-1}}$), we determined the hypocentres. In the first network setting (Network 1), 42 earthquakes were recorded in at least three stations. Fig. 6(a) shows the epicentres determined using the HYPO71 program with vertical error (erz) $\leq$0.4 km, horizontal error (erh) $\leq$0.4 km and rms arrival time residuals $\leq$0.035 s. A $\sim$20 km long, NW-SE oriented seismic fault is clearly observed. A cluster of activity is observed in the middle of the fault.

In the second SA network setting (Network 2), we recorded 66 earthquakes in at least three stations. Fig. 6(b) shows the epicentres with erz $\leq$ 0.35 km, erh $\leq$ 0.35 km and rms $\leq$ 0.035 s. In Fig. 6(a), the earthquakes tend to spread in the NW–SE direction. The cluster shown in Fig. 6(b) had an unclear NW–SE direction.

For the cluster in Fig. 6(b), we relocated 56 earthquakes with the HYPODD code (Fig. 6c), and the epicentral distribution suggests a NW–SE alignment that is almost equal to the one shown in Fig. 6(a). The Transbrasiliano lineament (Tl) cuts the study area in the NE–SW direction. Therefore, the earthquake sequence studied in this work has a roughly perpendicular direction to the Tl main alignment.

4.2 Fault-plane solutions

The fault-plane orientations and earthquake slip directions can provide us with important information regarding the geometry and structure of the fault at depth. A subset of 56 events in the Santana do Acaraú seismic sequence has similar waveforms. Repeated earthquakes present unique characteristics, and seismic sequences generated by a small area source are characterized by a highly similar waveform (e.g. Stabile *et al.* 2012).

Among the 56 events, we selected the 12 best-located events, which were better connected and recorded in at least four stations. These 12 earthquakes have rms residual $\leq$ 0.027 s, erz $\leq$ 0.30 km, erh $\leq$ 0.30 km and were used to estimate the fault plane orientation (azimuth and dip) with the least squares method.

The hypocentres of 12 events were distributed along a 2 km length (in surface) with depth varying between 3.5 and 4.6 km (Fig. 7).

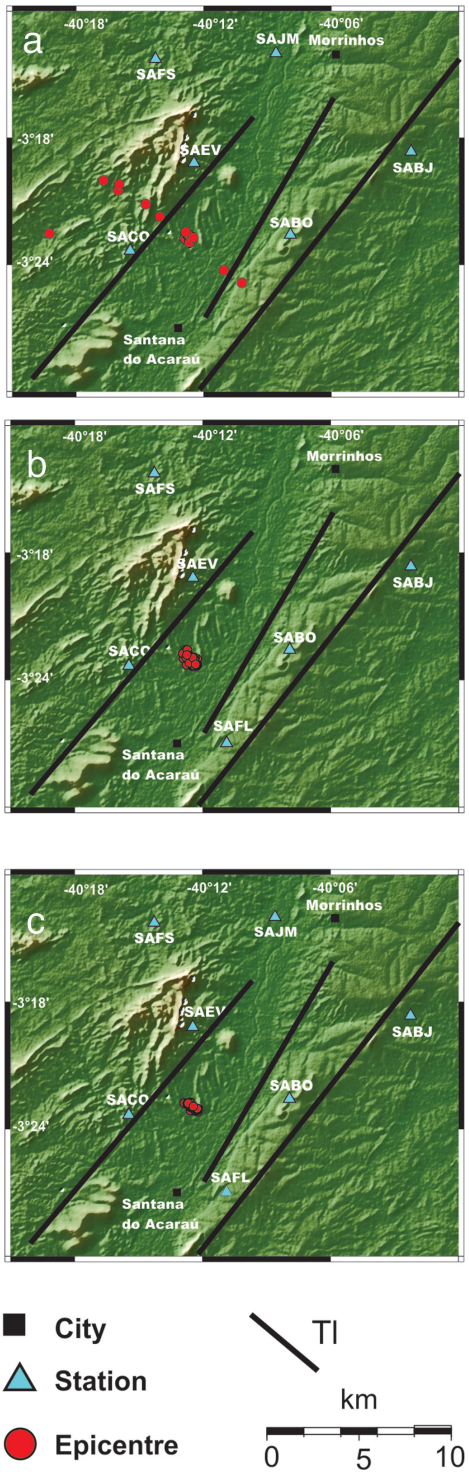

Figure 6. (a) Epicentral map of the first SA network (events from December 2009 to March 2010) showing 42 events (red circles) recorded by at least three stations with erz $\leq$ 0.4 km, erh $\leq$ 0.4 km and rms $\leq$ 0.035 s. Solid lines represent the Transbrasiliano lineament segments in the study area; (b) Epicentral map of the second SA network (October–December 2010) showing 66 events (red circles) recorded by at least three stations with erz $\leq$ 0.35 km erh $\leq$ 0.35 km and rms $\leq$ 0.035 s. Solid lines represent the Transbrasiliano lineament segments in the study area. Hypocentral locations determined by HYPO71 code; (c) Epicentral map of the 56 events (red circles) relocated using the hypoDD code showing the NW–SE alignment with erz $\leq$ 0.35 km erh $\leq$ 0.35 km and rms $\leq$ 0.035 s. Solid lines represent the Transbrasiliano lineament segments in the study area.

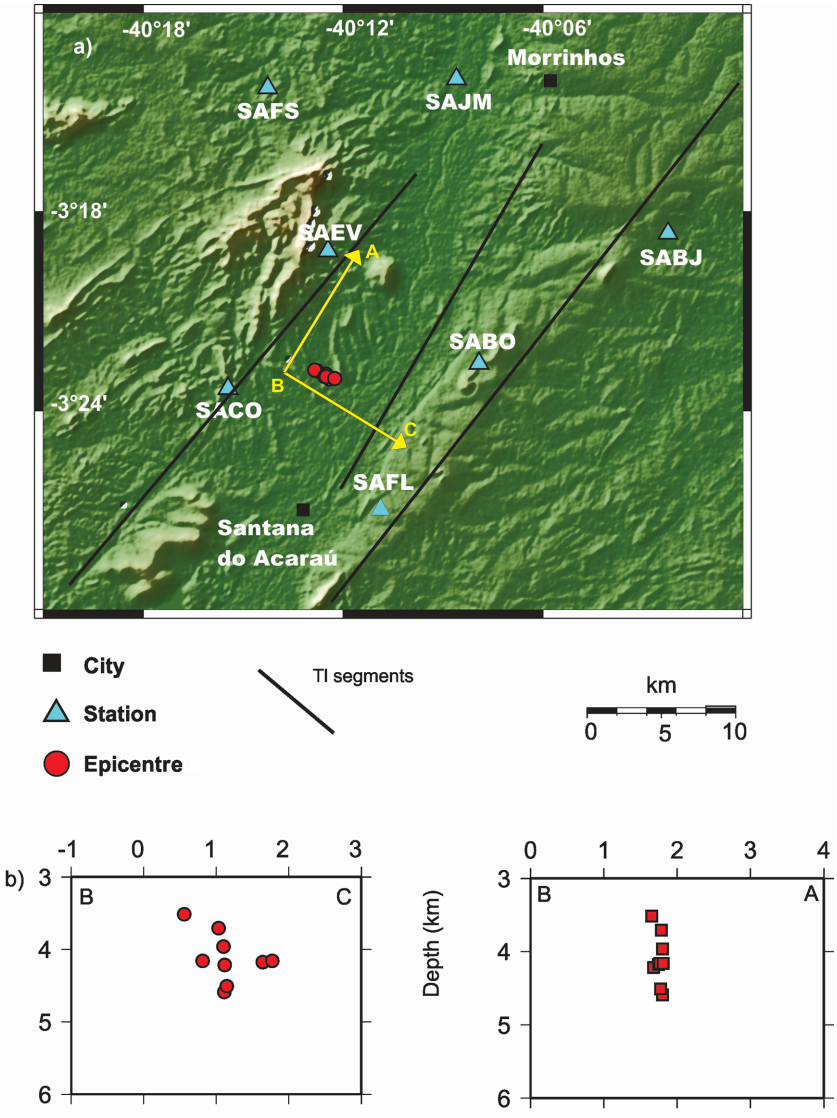

Figure 7. (a) Map of the 12 events (red circles) used to estimate the direction and dip of the fault plane. (b) Projections in the vertical planes perpendicular (BA) and parallel (BC) to the fault plane. Rms $\leq$ 0.027 s, erh $\leq$ 0.30 km and erz $\leq$ 0.30 km. Solid lines represent the Transbrasiliano lineament segments in the study area.

The fault plane has azimuth = 118° and dip = 86°. With these parameters, we performed a projection map of the hypocentres on the parallel and perpendicular directions to the fault plane (Fig. 7). These 12 events had 27 clear *P*-wave polarities, and we assumed that they were generated by the same source mechanism; they were selected to evaluate the focal mechanism.

We executed a grid search using the FPFIT program to find the best-fitting strike (S), dip (D) and rake (R). Considering the trend hypocenters observed in Fig. 7 and the best-fitting FPFIT solution corresponding to a fault plane with $S = 118°$ (fixed by the hypocentral distribution), we obtained $D = 85° \pm 5$ and $R = -15° \pm 10°$. Fig. 8 shows the preferred fault-plane solution with a strike-slip focal mechanism for the Santana do Acaraú seismic sequence. We named this active seismogenic fault the Santana Fault (SF).

4.3 Inversion of the focal mechanism

Previously, Ferreira *et al.* (1998) calculated the stress regime from focal mechanisms recorded at some seismographic networks deployed in the study area. Using four focal mechanisms, the inversion results indicated compressional maximum horizontal stress oriented in the 293° direction.

We updated the stress tensor of the ASZ by inserting new data into the existing dataset. The new data (Table 1) include the following three new focal mechanisms: (1) Senador Sá (França *et al.* 2004), (2) Serra da Meruoca (Oliveira *et al.* 2010) and (3) the new focal mechanism of Santana do Acaraú (this paper) (Table 1). We used the grid-search algorithm of Michael (1987). The advantage of using a focal mechanism to represent the average stress directions over other techniques is that they are more characteristic of the stress field at depth (Assumpção 1992; Ferreira *et al.* 1998).

Different focal mechanisms for the same region may result in different orientations of fault planes in the same uniform stress regime. To determine the average direction of the maximum horizontal compressive and the minimum horizontal compressive crustal stresses (σ_1 and σ_3 or SH_{max} and SH_{min}, respectively), we assumed that the stress field is uniform and that the principal stresses are oriented in the vertical and horizontal directions. Thus, we performed

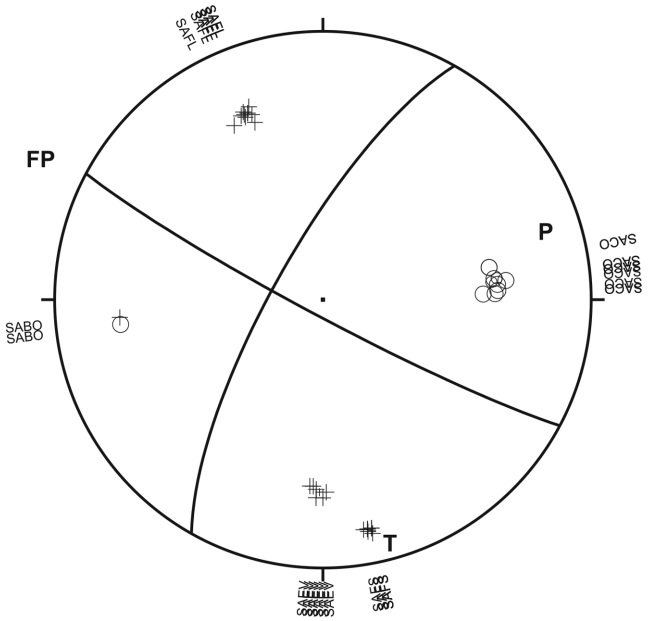

Figure 8. Composite focal mechanism using 12 selected events (Fig. 7) in the lower hemisphere, equal-area projection. FP represents the preferred fault plane. Circles and crosses represent the dilatational and compressional of *P* wave first arrivals, respectively. *P* and *T* indicate the tension and compression axes, respectively.

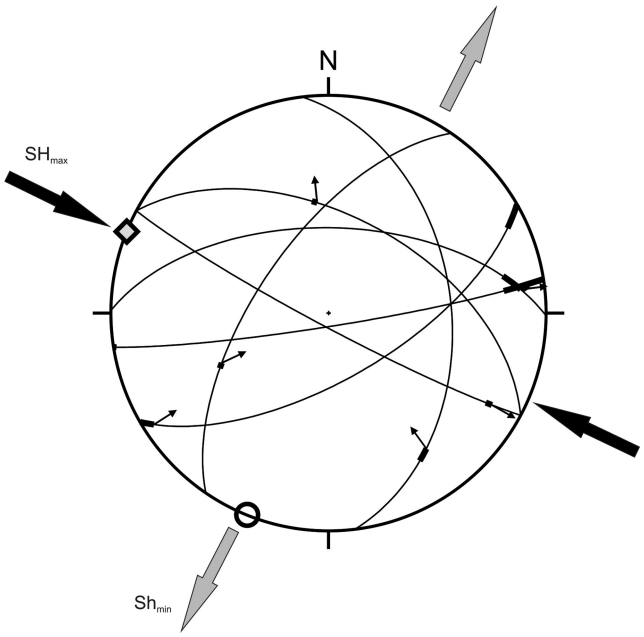

Figure 9. Stress tensor inversion of the seven focal mechanisms of Table 1. The closed and open arrows indicate the maximum horizontal stress direction ($\sigma_1 = SH_{max}$), and the minimum horizontal stress direction ($\sigma_3 = SH_{min}$), respectively. Thin solid lines are the fault planes with the observed slip vectors (small arrows) given by the fault plane solutions. The rake misfit is indicated by thick segment in the fault plane.

an inversion of focal mechanisms as used by Ferreira *et al.* (1998), Lopes *et al.* (2010) and Lima Neto *et al.* (2014).

Using seven focal mechanisms (Table 1), we found that a direction of 292° (Table 2) was the best fit for the compressive maximum horizontal stress direction (σ_1). The stress field was NW–SE-trending compression (σ_1), NE–SW-trending extension (σ_3) and σ_2 vertical (Fig. 9). The best-fitting shape factor ($\varphi = \frac{\sigma_2 - \sigma_3}{\sigma_1 - \sigma_3}$) was $\varphi = 0.4$ (Table 2).

The *P*-axes of focal mechanisms (Table 1) were approximately 206°, on average. Generally, the *P*-axes are not in the same direction as σ_1. However, we can use *P*-axes to infer the possible direction of the stress tensor (Zoback 1992; Assumpção 1998). Destro *et al.* (1994) found $\sigma_1 = 280°$ using structural geology methods (fault-slip data) for local stress in the vicinity of the Santana do Acaraú town, which differs 12° from the value found in this paper. However, one difference is that we evaluated the regional stress. Information obtained from hypocentres aided in determining the Santana fault plane direction and demonstrates that our results are reliable (Lima Neto *et al.* 2014). The stress tensor uncertainties (ers in Table 2) were estimated using a grid search with a few of tens of resamples that were randomly chosen from the fault-plane parameters (S, D and R), as described by Lima Neto *et al.* (2014).

5 DISCUSSION: STRESS FIELD AND SEISMICITY ALONG THE EQUATORIAL MARGIN

5.1 The role of pre-existing structures in the seismicity

In this section, we focus on the origin of the seismicity in continental margins. Many examples of structural reactivation of pre-existing faults and ductile fabrics, such as shear zones, have been cited to explain the important role of localizing deformation and fault reactivation (Holdsworth *et al.* 1997). This mechanism has been used to explain the intraplate seismicity (Sykes 1978). This is the case for the central part of the Borborema province, where seismogenic faulting reactivates a pre-existing continental-scale ductile shear zone, the Pernambuco lineament (Ferreira *et al.* 2008; Lopes *et al.* 2010; Lima Neto *et al.* 2013).

However, other studies indicated that intraplate seismicity could not be related to a single causal mechanism (Mazzotti 2007; Talwani 2014). While many examples indicate that reactivation of pre-existing structures plays an important role in the tectonic evolution of the continents and intraplate seismicity, there has been considerably less attention on cases in which there is no reactivation of pre-existing structures. These cases are also important to our understanding of intraplate seismicity (Sandiford & Egholm 2008).

Table 2. Results of seven focal mechanisms inversion. The main stresses from the Acaraú seismic zone area were constrained to be horizontal and vertical. Ers is an estimate of the uncertainties in the σ_1, σ_2 and σ_3 orientations. ϕ is the shape factor. *N* is the number of focal mechanism used. Misfit angle is the difference between the observed slip and the shear stress in the fault plane. a, azimuth; p, plunge.

σ_1 (a/p/ers)	σ_3 (a/p/ers)	σ_2 (a/p/ers)	ϕ	*N*	Misfit angle range
292/0/±9°	202/0/±8°	Vertical	0.4 ± 0.1	7	1°–21°

The results of this study indicate that most faults in the Acaraú seismic zone cut across the pre-existing fabric (Ferreira *et al.* 1998; França *et al.* 2004). This includes the NE–SW-striking Santana fault, which is orthogonal to a ductile shear zone and its brittle reactivation along the Transbrasiliano lineament (Fig. 6). Although fault reactivation occurred during the Cambrian–Devonian on the formation of the Jaibaras basin (Oliveira & Mohriak 2003) and, more recently, in the Meruoca Granite (Moura *et al.* 2014), fault reactivation does not explain most of the present-day seismicity in the area.

5.2 The influence of the continental margin in the stress field and seismicity

The focal mechanism and resulting inversion findings indicate that the maximum compressive stress (σ_1) is also parallel to the continental margin in the NW part of the Borborema province. This result is in agreement with previous focal mechanism data (Assumpção 1992; Ferreira *et al.* 1998) and image logs (Reis *et al.* 2013) in the Potiguar basin and its host Precambrian basement. This pattern also continues to the west as far as the Amazon fan, where the focal mechanisms are roughly parallel to the continental margin (Lima *et al.* 1997).

Two major causes have been cited to explain the maximum compressive stress (or the maximum horizontal stress) parallel to the continental margin. First, the strike-slip focal mechanisms and seismicity indicate that the stress pattern along this part of the Equatorial margin is the result of a combination of plate-wide forces (asthenospheric drag or ridge-push) with local sources (density contrasts between oceanic and continental crusts; Assumpção 1992). This would cause flexural stresses in which the maximum horizontal compression is parallel to the margin in a superposition of regional (ridge push and astenospheric drag) and local stresses (effect of the margin; Assumpção 1992; Ferreira *et al.* 1998). By contrast, in the Amazon fan area, approximately 900 km west of the study area, borehole breakout data parallel to the margin were explained as being the result of flexural stresses due sediment loading. The superposition of these sediments on a strong, dense and cold lithosphere would create flexural stresses that would extend for some hundreds of kilometres inland (Watts *et al.* 2009). Flexure due to sediment loading might also manifest in faulting and seismicity patterns (Watts *et al.* 2009). We suggest that both explanations are complementary because the sedimentary pile reached at least 10 km since the Miocene in the Amazon area, whereas the sediment load is less than 2–3 km along the Equatorial margin in the Borborema province.

One final explanation for the maximum compressive stress parallel to the margin is associated with the thermal influence of a hot oceanic crust in contrast with the relatively cold continental crust. Numerical simulations of the Australian stress field indicated that the thermal structuring associated with lateral heat flow along continental margins could result in mechanical weakening of the continental interiors. This could make the maximum compressive stress parallel to the margin and influence the distribution of seismicity around the continental margin (Sandiford & Egholm 2008). This final explanation could also have contributed to the seismicity and pattern of the stress field observed in our study area. However, because there are no available thermal data along the Equatorial margin of Brazil, we suggest that this thermal component should be investigated in future studies.

6 CONCLUSIONS

The focal mechanisms and relocated hypocentres of the Santana do Acaraú earthquake sequence clearly reveal a previously unknown strike-slip fault (the Santana Fault) with a NW–SE orientation, at a 3–4.5 km depth, with a ∼5 km length. This seismogenic fault cuts across major ductile shear zones and associated brittle reactivations.

The different focal mechanisms evaluated in the Acaraú seismic zone, the NW part of the Borborema province, are consistent with a uniform strike-slip stress tensor with roughly NW–SE maximum horizontal compression ($SH_{max} = 292^{\circ}$) and SW–NE minimum compression. The newly focal mechanism and stress inversion shown in this paper are in agreement with previous studies that suggested $SH_{max} = 293^{\circ}$ and NW–SE-trending to the SH_{max} orientation. The SH_{max} is parallel to the margin. We suggest that the continental margin influences this stress pattern, which may have implications for the entire Equatorial margin of Brazil.

Several intraplate seismic zones in the world and in the Borborema province have been investigated, and their characteristics have been described. Although several studies have attempted to explain intraplate seismicity, a general correlation or single model has not yet been identified. The seismicity pattern recorded in the study area occurs in earthquake sequences that last several years and with magnitudes up to 4.9 m_b.

ACKNOWLEDGEMENTS

We thank Lucas Vieira Barros, an anonymous reviewer, and the GIJ editor for their comments and corrections, which greatly improved our work. This study was sponsored by the Brazilian National Research Council (CNPq) INCTET Project no. 573713/2008-1, coordinated by Reinhardt A. Fuck (Universidade de Brasília). This work also benefited from the Pool of Geophysical equipment of Brazil coordinated by the Observatório Nacional (ON, Rio de Janeiro, Brazil). JMF, FHRB, AFN and MA thank CNPq for their research grants. PHSO thanks CAPES-Brazil for his PhD grant.

REFERENCES

Assumpção, M., 1992. The regional intraplate stress field in South America, *J. geophys. Res.,* **97**(B8), 11 889–11 903.

Assumpção, M., 1998. Seismicity and stress in the Brazilian passive margin, *Bull. seism. Soc. Am.,* **88**(1), 160–169.

Assumpção, M. *et al.*, 2014. Intraplate seismicity in Brazil, in *Intraplate Seismicity,* pp. 50–71, ed. Talwani, P., Cambridge Univ. Press.

Bezerra, F.H.R., Takeya, M.K., Sousa, M.O.L. & do Nascimento, A.F., 2007. Coseismic reactivation of the Samambaia fault, Brazil, *Tectonophysics,* **430,** 27–39.

Bezerra, F.H.R., do Nascimento, A.F., Ferreira, J.M., Nogueira, F.C., Fuck, R.A., Brito Neves, B.B. & Souza, M.O.L., 2011. Review of active faults in the Borborema Province, Intraplate South America—integration of seismological and paleoseismological data, *Tectonophysics,* **510,** 269–290.

Brito Neves, B.B., Fuck, R.A. & Pimentel, M.M., 2014. The Brasiliano Collage in South America: a review, *Braz. J. Geol.,* **44,** 493–518.

De Castro, D.L., Fuck, R.A., Phillips, J.D., Vidotti, R.M., Bezerra, F.H.R. & Dantas, E.L., 2014. Crustal structure beneath the Paleozoic Parnaíba basin revealed by airborne gravity and magnetic data, Brazil, *Tectonophysics,* **614,** 128–145.

DeMatos, R.M., 1992. The northeast Brazilian rifts system, *Tectonics,* **11,** 766–791.

DeMatos, R.M., 2000. Tectonic evolution of the Equatorial South Atlantic, in *Atlantic Rifts and Continental Margins,* pp. 331–354, eds Mohriak, W. & Taiwani, M., American Geophysical Union.

Destro, N., Szatmari, P. & Ladeira, E.A., 1994. Post-Devonian transpressional reactivation of a Proterozoic ductile shear zone in Ceará, Brazil, *J. Struct. Geol.,* **16**(1), 33–35.

Ferreira, J.M. & Assumpção, M., 1983. Sismicidade do Nordeste do Brasil, *Rev. Bras. Geof.,* **1,** 67–88.

Ferreira, J.M., Oliveira, R.T., Takeya, M.K. & Assumpção, M., 1998. Superposition of local and regional stresses in NE Brazil: evidence from local mechanisms around the Potiguar marginal basin, *Geophys. J. Int.,* **134,** 341–355.

Ferreira, J.M., Bezerra, F.H.R., Sousa, M.O.L., Nascimento, A.F. & França, G.S.L.A., 2008. The role of Precambrian mylonitic belts and present-day stress field in the coseismic reactivation of the Pernambuco lineament, Brazil, *Tectonophysics,* **456,** 111–126.

Fetter, A.H., Van Schmus, W.R., dos Santos, T.J.S., Arthaud, M.H. & Nogueira Neto, J.A., 1997. Geologic history and framework of Ceará State: northwest Borborema Province, NE Brazil, in *Proceedings of the South American Symposium on Isotope Geology,* Brazil, Extended Abstracts, pp. 112–114.

França, G.S., Ferreira, J.M. & Takeya, M.K., 2004. Seismic activity in Senador – Sá, Brazil. 1997–1998, *Rev. Bras. Geof.,* **22,** 115–125.

Holdsworth, R.E., Butler, C.A. & Roberts, A.M., 1997. The recognition of reactivation during continental deformation, *J. Struct. Geol.,* **154,** 73–78.

Johnston, A.C., 1989. The seismicity of stable continent interior, in *Earthquake at North-Atlantic Passive Margins: Neotectonics and Postglacial Rebound,* pp. 299–327, eds Gregersen, S. & Basham, P.W., Kluwer Academic.

Lee, W.H.K. & Lahr, J.C., 1975. HYPO71 (revised): a computer program for determining hypocenter, magnitude and first motion pattern of local earthquakes, *U.S. Geol. Surv. Open File Rep.,* pp. 75–311.

Lima Neto, H.C., Ferreira, J.M., Bezerra, F.H.R., Assumpção, M., do Nascimento, A.F., Sousa, M.O.L. & Menezes, E.A.S., 2013. Upper crustal earthquake swarms in São Caetano: reactivation of the Pernambuco shear zone and trending branches in intraplate Brazil, *Tectonophysics,* **633,** 211–220.

Lima Neto, H.C., Ferreira, J.M., Bezerra, F.H.R., Assumpção, M., do Nascimento, A.F., Sousa, M.O.L. & Menezes, E.A.S., 2014. Earthquake sequences in the southern block of the Pernambuco Lineament, NE Brazil: stress field and seismotectonic implications, *Tectonophysics,* **608,** 804–811.

Lima, C.C., Nascimento, E. & Assumpção, M., 1997. Stress orientations in Brazillian sedimentary basins from breakout analysis—implications for force models in the South American plate, *Geophys. J. Int.,* **130,** 112– 24.

Lopes, A.E.V., Assumpção, M., do Nascimento, A.F., Ferreira, J.M., Menezes, E.A.S. & Barbosa, J.R., 2010. Intraplate earthquake swarm in Belo Jardim, NE Brazil: reactivation of a major Neoproterozoic shear zone (Pernambuco Lineament), *Geophys. J. Int.,* **180,** 1303–1312.

Mazzotti, S., 2007. Geodynamics models for earthquake studies in intraplate North America, *GSA Spec Papers,* **425,** 17–33.

Michael, A.J., 1984. Determination of stress from slip data: fault and folds, *J. geophys. Res.,* **89,** 1517–1526.

Michael, A.J., 1987. Use of focal mechanisms to determine stress: a control study, *J. geophys. Res.,* **92,** 357–368.

Moura, A.C.A., Oliveira, P.H.S., Ferreira, J.M., Bezerra, F.H.R., Fuck, R.A. & do Nascimento, A.F., 2014. Brittle tectonics and seismicity in the Meruoca Granite, NW Ceará, Borborema Province, *Ann. Braz. Acad. Sci.,* **86**(4), 1631–1639.

Oliveira, D.C. & Mohriak, W.U., 2003. Jaibaras trough: an important element in the early tectonic evolution of the Parnaíba Interior Sag Basin, Northern Brazil, *Mar. Petro. Geol.,* **20,** 351–283.

Oliveira, P.H.S., Ferreira, J.M., do Nascimento, A.F., Bezerra, F.H.R., Soares, J.E. & Fuck, R.A., 2010. Study of the Sobral seismicity, NE Brazil, in 2008, in *Proceedings of IV Geophysics Brazilian Symposium,* Brasília, Brazil.

Reasenberg, P. & Oppenheimer, D., 1985. FPFIT, FPPLOT and FPPAGE: Fortran computer programs for calculating and displaying earthquake fault-plane solutions, *U.S. Geol. Surv.,* pp. 85–739.

Reis, A.F.C., Bezerra, F.H.R., Ferreira, J.M., Nascimento, A.F. & Lima, C.C., 2013. Stress magnitude and orientation in the Potiguar basin, Brazil: implications on faulting style and reactivation, *J. geophys. Res.,* **118,** 5550–5563.

Sandiford, M. & Egholm, D.L., 2008. Enhanced intraplate seismicity along continental margins: some causes and consequences, *Tectonophysics,* **457,** 197–208.

Santos, T.J.S., Fetter, A.H, Hackspacher, P.C. & Nogueira Neto, J.A., 2008. Neoproterozoic tectonic and magmatic episodes in the NW sector of Borborema Province, NE Brazil, During Assembly of Western Gondwana, *J. S. Am. Earth Sci.,* **25,** 271–284.

Stabile, T.A., Satriano, C., Orefice, A., Festa, G. & Zollo, A., 2012. Anatomy of a microearthquake sequence on an active normal fault, *Sci. Rep.,* **2,** 410.

Sykes, L.R., 1978. Intraplate seismicity, reactivation of preexisting zones of weakness, alkaline magmatism, and other tectonism postdating continental fragmentation, *Rev. Geophys. Space Phy.,* **16,** 621–688.

Talwani, P., 2014. *Intraplate Earthquakes,* Cambridge Univ. Press, 398 pp.

Van Arsdale, R., 2014. The New Madrid seismic zone of the Central United States, in *Intraplate Seismicity,* pp. 162–197, ed. Talwani, P., Cambridge Univ. Press.

Waldhauser, F., 2001. HYPODD—a program to compute double-difference hypocenter locations, US Geological Survey Open-File Report, pp. 01–113.

Waldhauser, F. & Ellsworth, W.L., 2000. A double – difference earthquakes location algorithm: method and application to the Northern Hayward Fault, California, *Bull. seism. Soc. Am.,* **90,** 1353–1368.

Watts, A.B., Rodger, M., Pierce, C., Greenroyd, C.J. & Hobbs, R.W., 2009. Seismic structure, gravity anomalies, and flexure of the Amazon continental margin, NE Brazil, *J. geophys. Res.,* **114**(B7), doi:10.1029/2008JB006259.

Zoback, M.L., 1992. Stress filed constraint on intraplate seismicity in eastern North America, *J. geophys., Res.,* **97,** 11 761–11 782.